



Cite this: DOI: 10.1039/d5cc06007a

Received 22nd October 2025,
Accepted 20th November 2025

DOI: 10.1039/d5cc06007a

rsc.li/chemcomm

Biochar-supported Cu catalyst for low-temperature base-free oxidative *N*-formylation of amines with paraformaldehyde in green solvent

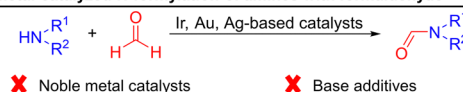
Haihua Yin,^{ab} Zhenjie Wang,^{ab} Hangkong Yuan^{*a} and Xingchao Dai^{ib} ^{*a}

A novel cellulose-biochar-supported copper catalyst enables base-free oxidative *N*-formylation of amines with paraformaldehyde in green H₂O solvent at 50 °C. This green protocol efficiently converts diverse amines into formamides, including pharmaceutical intermediates, via a radical mechanism co-mediated by [•]OH and [•]OOH species.

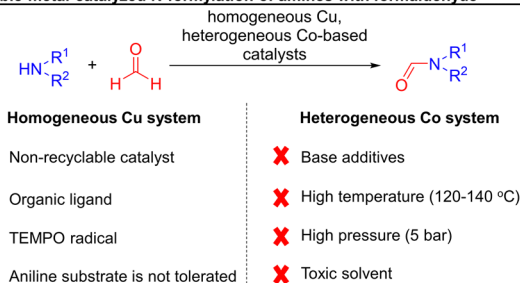
Formamides, constituting an important class of the amide family, have been widely used in various roles: as an important industrial solvent in the case of *N,N*-dimethylformamide (DMF),¹ synthetic intermediates in the preparation of fungicides and pharmaceuticals,² a protective group³ and a catalyst in certain reactions.⁴ Due to their wide applications, intense efforts have been made to develop clean and sustainable methods for synthesizing them.⁵ Based in part on whether any reductants or oxidants are involved, these developed methods can be divided into three classes: (1) “neutral” *N*-formylation of amines with carbonyl-containing molecules such as monoxide (CO),⁶ formic acid and its derivatives,⁷ DMF;⁸ (2) reductive *N*-formylation of amines or nitro-compounds with carbon dioxide (CO₂),⁹ in which reductants are required to reduce CO₂ and/or nitro-compounds; (3) oxidative *N*-formylation of amines with methanol,¹⁰ formaldehyde,¹¹ non-C1 molecules containing C–C/C=C bonds,^{12,13} in which oxidants are necessary for the selective oxidation of methanol and formaldehyde, and selective oxidative cleavage of C–C/C=C bonds in non-C1 molecules. Of these methods, the oxidative protocol in particular has attracted increasing attention due to its mild reaction conditions, avoiding the use of expensive and explosive hydrogen gas (H₂), and replacing highly toxic CO with a green and safe carbonyl source.

Many carbonyl sources, including methanol, formaldehyde and its analogues, glycerol and its derivatives, and others, have been applied to the oxidative *N*-formylation of amines to formamides.¹⁴ The oxidative *N*-formylation of amines with formaldehyde as the carbonyl source is a particularly attractive method due to the inexpensive and wide availability of the raw materials, and water being the only by-product. Since the pioneering works of Friend¹⁵ and Madi,¹⁶ in which metallic gold and silver were used to catalyze oxidative *N*-formylation of amines with formaldehyde, a series of noble-metal-based catalysts based on Ir¹⁷ and Au^{18–22} have been successfully developed (Scheme 1a). However, the use of costly noble metals and basic additives poses an obstacle for their further application. Recently, two examples of non-noble-metal catalysts, namely

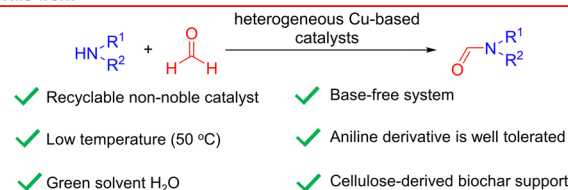
a) Noble-metal-catalyzed *N*-formylation of amines with formaldehyde



b) Non-noble-metal-catalyzed *N*-formylation of amines with formaldehyde



c) This work


Scheme 1 *N*-Formylation of amines with formaldehyde.

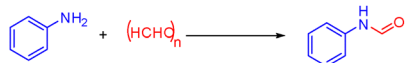
^a State Key Laboratory of Low Carbon Catalysis and Carbon Dioxide Utilization Lanzhou Institute of Chemical Physics, Chinese Academy of Sciences, No. 18, Tianshui Middle Road, Lanzhou, 730000, China. E-mail: yuanhk@licp.cas.cn, daixingchao@licp.cas.cn

^b University of Chinese Academy of Sciences, No. 19 A, Yuquanlu, Beijing, 100049, China

Cu complex and CoNC catalysts, were reported by Precht²³ and Ke,²⁴ respectively (Scheme 1b). However, the former is a homogeneous system and suffers from difficulty in the recyclability of the catalysts, the use of expensive organic ligands, base additives and 2,2,6,6-tetramethylpiperidine-*N*-oxyl (TEMPO) co-catalyst, as well as no activity for aniline substrates. Although the latter is recyclable, it has some obvious drawbacks such as the harsh reaction conditions (high reaction temperature and pressure) and the use of base additives and toxic solvents. Therefore, it is highly desirable to develop a mild and base-free protocol for synthesizing formamides from amines and formaldehyde over a heterogeneous, inexpensive metal catalyst in a green reaction medium. Considering these issues, here we developed a mild and base-free system for the oxidative *N*-formylation of amines with paraformaldehyde over cellulose-derived biochar-supported copper catalyst in green H₂O solvent at 50 °C (Scheme 1c). To the best of our knowledge, this is the first non-noble-metal base-free catalytic system.

Three biochar-supported copper catalysts with a theoretical Cu content of 2 wt% were prepared with CuCl₂·2H₂O as the metal precursor and three biochars derived from, respectively, cellulose acetate (CA), ethyl cellulose (EC), and carboxymethyl cellulose (CMC) as supports. Their catalytic performance was evaluated using oxidative *N*-formylation of aniline with paraformaldehyde and H₂O₂ oxidant as the model reaction at 50 °C in H₂O solvent. To our delight, when using Cu/CA as the catalyst, formanilide was obtained with a yield of 71% after reaction for 8 h (Table 1, entry 1). Lower yields of 66% and 55% were obtained when using, respectively, Cu/EC (entry 2) and Cu/CMC (entry 3) instead of Cu/CA. Using a commercial active carbon (AC)-supported copper catalyst, denoted as Cu/AC, as a reference catalyst gave a 64% yield (entry 4), lower than that for Cu/CA, indicating the superiority of the cellulose-derived biochar support. A yield of only 38% was obtained without a catalyst (entry 5), suggesting the necessity of the catalyst for good activity. Bare CA support gave nearly the same yield as did the case without catalyst (entry 6), indicative of a lack of activity of CA for the reaction and that the improved activity derived from the supported Cu. Several ratios of aniline to paraformaldehyde were tested, and a value of 1.5 : 1 gave the best yield of 80% (entries 1 and 7–9). Testing various amounts of H₂O₂ from 1 to 3 mmol showed the highest yield when using 2 mmol H₂O₂ (entries 7 and 10–11). No product was observed without H₂O₂, suggesting an inability of the catalyst to activate air/O₂ as the oxidant (entry 12); further evidence for this conclusion was provided by the results of a control experiment with 5 bar O₂ as the oxidant (entry 13). The yield obtained for a reaction time of 8 h was higher than those for shorter and longer reaction times (entries 7 and 14–15). Similar reductions in yield were observed when varying the reaction temperature (entries 16 and 17) and H₂O amount (entries 18 and 19) and catalyst (entries 20 and 21) from the above-described ones (entry 7). Reducing the Cu content to 1 wt% lowered the yield from 80% to 45% (entries 7 and 22), while increasing the Cu content to 4 wt% led to a slight decrease in the yield (entries 7 and 23). Under the optimized reaction conditions, alongside formamide products,

Table 1 Catalyst screening and optimization of reaction conditions^a



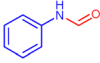
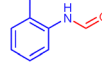
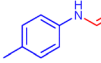
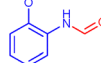
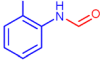
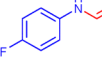
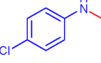
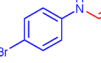
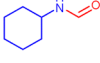
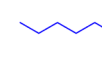
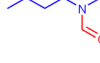
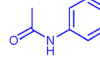
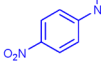
Entry	Catalyst	Aniline (mmol)	(HCHO) _n (mmol)	H ₂ O ₂ (mmol)	Yield ^b (%)
1	Cu/CA	2	1	2	71
2	Cu/EC	2	1	2	66
3	Cu/CMC	2	1	2	55
4	Cu/AC	2	1	2	64
5	—	2	1	2	38
6	AC	2	1	2	39
7	Cu/CA	1.5	1	2	80
8	Cu/CA	1	1.5	2	59
9	Cu/CA	1	1	2	56
10	Cu/CA	1.5	1	3	63
11	Cu/CA	1.5	1	1	43
12	Cu/CA	1.5	1	0	0
13 ^b	Cu/CA	1.5	1	0	0
14 ^c	Cu/CA	1.5	1	2	77
15 ^d	Cu/CA	1.5	1	2	68
16 ^e	Cu/CA	1.5	1	2	29
17 ^f	Cu/CA	1.5	1	2	67
18 ^g	Cu/CA	1.5	1	2	61
19 ^h	Cu/CA	1.5	1	2	67
20 ⁱ	Cu/CA	1.5	1	2	47
21 ^j	Cu/CA	1.5	1	2	66
22	1 wt%Cu/CA	1.5	1	2	45
23	4 wt%Cu/CA	1.5	1	2	77
24 ^k	Cu/CA	1.5	1	2	66
25 ^l	Cu/CA	1.5	1	2	86

^a Reaction conditions: 2 mmol aniline, 30 mg paraformaldehyde (1 mmol HCHO), 2 mmol H₂O₂ (35 wt%), 25 mg catalyst, 1 mL solvent, 50 °C (oven temperature), 8 h. Yields were determined using GC-FID with toluene as an external standard. ^b O₂ 5 bar. ^c 6 h. ^d 12 h. ^e 30 °C. ^f 60 °C. ^g 0.5 mL H₂O. ^h 2 mL H₂O. ⁱ 10 mg catalyst. ^j 40 mg catalyst. ^k Formaldehyde aqueous solution. ^l With catalyst recovered from a previous run.

imines and aniline oxidation by-products such as azobenzene and azoxybenzene were observed. Notably, our system was also found to be active with formaldehyde (dissolved in water) as the carbonyl source and a 66% yield was found under the optimized reaction conditions (entry 24). Delightfully, our catalyst was found to be reusable: good catalytic activity was also displayed by the catalyst recovered using simple filtration, washing and drying without further activation treatment (entry 25).

With the active catalyst Cu/CA in hand, the scope of amine substrates and tolerance of our catalytic system to various functional groups were studied (Table 2). Our system clearly showed good functional group tolerance: aniline and its derivatives substituted with electron-donating groups such as Me- and MeO- and electron-withdrawing ones such as F-, Cl-, and Br- were converted into the corresponding formamide products in moderate to good yields. Except for aromatic amines, our system was also found to be active for aliphatic amine substrates. Yields of 57–82% were obtained with, respectively, cyclohexylamine, 1-octylamine and dibutylamine as substrates. Moreover, *N*-(4-acetylphenyl)-formamide and 4-(4-nitrophenyl)piperazine-1-carbaldehyde, two important intermediates for the synthesis of the antibacterial agent oxazolidinone, were synthesized using our protocol in 73% and 67% yields, respectively.

Table 2 *N*-Formylation of various amines with paraformaldehyde^a

			
80 %	66 % ^b	75 % ^b	84 % ^c
			
69 % ^c	69 % ^c	75 % ^{c,d}	65 % ^{c,d}
			
82 % ^e	57 % ^f	65 % ^f	
			
73 % ^g	67 % ^h		

^a Reaction conditions: 2 mmol amine, 30 mg paraformaldehyde (1 mmol HCHO), 2 mmol H₂O₂ (35 wt%), 25 mg Cu/CA catalyst, 1 mL H₂O, 50 °C (oven temperature), 8 h. Yields were determined using GC-FID with toluene as an external standard. ^b H₂O₂ 2.25 mmol, 12 h. ^c 24 h. ^d H₂O 2 mL. ^e Cyclohexylamine 2 mmol, H₂O₂ 1 mmol, DMF 1 mL, 12 h. ^f 1-Octylamine 5 mmol, H₂O₂ 6 mmol, 80 °C, 12 h. ^g DMF 2 mL, 24 h. ^h *N*-Methylpyrrolidone (NMP) 2 mL, 12 h.

To relate activity to structure, the active catalyst Cu/CA was fully characterized. The Cu content was determined using an atomic absorption spectrometer (AAS) to be 2.8 wt% (Table S1). N₂ adsorption and desorption analysis showed a BET surface area of 652.6 m² g⁻¹, total pore volume of 0.6642 cm³ g⁻¹ and average pore radius of 2.0 nm for the biochar CA support, and similar values for the support with Cu (Table S1 and Fig. S1). The XRD pattern of the Cu/CA catalyst showed two broad diffraction peaks in the 2θ ranges 20–30° and 40–50° (Fig. 1a), which can be attributed to, respectively, (002) and (100) planes of carbon.²⁵ Three sharp diffraction peaks, at 2θ = 36.4, 43.3 and 50.4°, were also observed, and were assigned to CuCl (200), Cu (111) and Cu (200) (PDF#30-0472 and PDF#85-1326). The formation of CuCl species was further confirmed by the results in the Cl 2p region of the XPS spectrum of the catalyst (Fig. 1b). The Cu 2p region of its spectrum showed no typical satellite peak around 945 eV (Fig. 1c), suggesting the absence of Cu^{II} species on its surface. This region did show a main signal peak centered at 932.9 eV, which can be assigned to the Cu^{I/0} species. To distinguish the Cu^{I/0} species, a Cu LMM Auger spectrum of the catalyst was recorded (Fig. 1d). Fitting analysis revealed two sub-peaks at 918.0 and 916.0 eV, corresponding to Cu^I and Cu⁰ species, respectively.²⁶ By integrating the areas of these sub-peaks, the relative amounts of surface Cu consisting of Cu^I and metal Cu⁰ species were determined to be 76% and 24%, respectively, with this co-existence of Cu⁰ and Cu^I species on the surface being quite consistent with the XRD results. A high-angle annual dark-field (HAADF)-scanning transmission electron microscopy (STEM) image of fresh Cu/CA catalyst showed nanoparticles of different sizes (Fig. S2a). The corresponding energy-dispersive spectroscopy (EDS) elemental mapping confirmed the

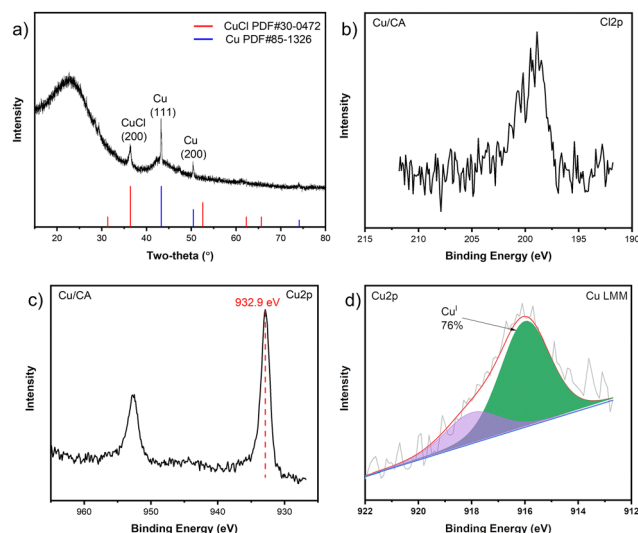


Fig. 1 (a) XRD pattern, (b) Cl 2p, (c) Cu 2p and (d) Cu LMM Auger XPS spectra of the Cu/CA catalyst.

presence of inhomogeneously mixed Cu and Cl (Fig. S2b–f), suggesting the presence of other Cu-containing species in addition to CuCl species.

To derive a possible mechanism for the overall reaction, the model reaction was tracked using GC-MS. Here, the imine *N*-phenylmethanimine was observed. To confirm a possible role of *N*-phenylmethanimine as a reaction intermediate, the control experiment without H₂O₂ was performed (Fig. S3a). After reaction for 4 h, only *N*-phenylmethanimine was observed. Then, a quantity of 2 mmol H₂O₂ was added to the reaction mixture, and reacted for another 4 h. Here, a yield of only 47% was obtained, lower than the 66% yield obtained with the same reaction time under the optimized reaction conditions (Fig. S3a vs. S3b), and hence suggestive of *N*-phenylmethanimine not being an intermediate. Considering the possible oxidation of formaldehyde to formic acid (HCOOH), the control experiment with HCOOH as the carbonyl source was performed (Fig. S3c). The results showed that only a trace amount of formanilide product was generated, basically excluding the possibility of HCOOH as the reaction intermediate. As Cu-based catalyst has been reported to be able to activate H₂O₂ to form reactive radical species, such as •OH and •OOH, control experiments were performed using *tert*-butyl alcohol (*t*-BuOH), a selective radical scavenger for •OH,²⁷ and *p*-benzoquinone,²⁸ a selective scavenger for O₂^{•-}, a species easily converted to •OOH radicals. The results showed that the addition of *t*-BuOH reduced the formamide product yield from 80% to 69% (Fig. S3d), suggesting a role for •OH radicals in the formation of formamide product. A more pronounced inhibition effect was observed when adding *p*-benzoquinone to the reaction, with the yield here dropping to 42% (Fig. S3e), indicative of •OOH radicals behaving as the main reactive oxygen species in the reaction with •OH radicals playing a minor role. To confirm the existence of •OH and •OOH radicals and exclude the possible effect of H₂O₂ decomposition resulting from the reaction temperature, an electron paramagnetic resonance (EPR) spin trapping

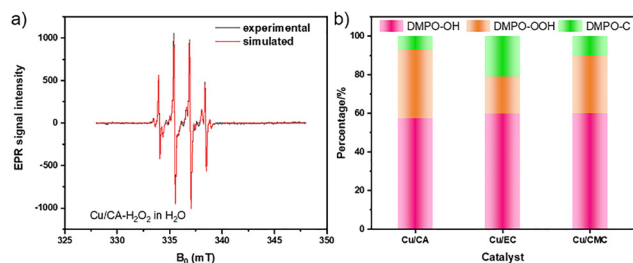


Fig. 2 (a) Experimental and fitted EPR spectra of DMPO spin adducts. For fitting, the following hfs parameters were used:²⁹ $A_N = 14.9$, $A_H = 14.5$ for $\bullet\text{OH}$, $A_N = 14.1$, $A_{\text{BH}} = 11.2$, $A_{\text{YH}} = 1.3$ for $\bullet\text{OOH}$ and $A_N = 15.4$, $A_H = 22.7$ for $\bullet\text{C}$. (b) Plot of the relative amounts of DMPO spin adducts.

experiment with 5,5-dimethyl-1-pyrroline-*N*-oxide (DMPO) was conducted at room temperature. For Cu/CA catalyst mixed with H_2O_2 in H_2O at room temperature, signals for DMPO-OH, DMPO-OOH and DMPO-C adducts were observed (Fig. 2a), indicating the formation of $\bullet\text{OH}$, $\bullet\text{OOH}$ and $\bullet\text{C}$ radicals. Similar results were observed with Cu/EC and Cu/CMC catalysts (Fig. S4). The $\bullet\text{OH}$ and $\bullet\text{OOH}$ species apparently resulted from the activation of H_2O_2 over Cu/CA catalyst, while the $\bullet\text{C}$ species may have been from the interaction between reactive radical species and the biochar support. Further simulation analysis revealed relative amounts of 57.3%, 35.7% and 7% for $\bullet\text{OH}$, $\bullet\text{OOH}$ and $\bullet\text{C}$ radicals, respectively (Fig. 2b). When changing the catalyst to Cu/EC and Cu/CMC, the proportion of $\bullet\text{OOH}$ radicals was lower than that for Cu/CA (Fig. 2b), perhaps explaining the lower activities of Cu/EC and Cu/CMC than of Cu/CA. This result was also consistent with the control experiment result of $\bullet\text{OOH}$ radicals being the main reactive oxygen species.

Based on the above results and previous literature,^{22,23} a possible reaction mechanism was proposed (Fig. S5). First, when paraformaldehyde is dissolved in H_2O solvent under heating, formaldehyde is released, which then reacts with amine substrate to form the hemiaminal intermediate over Cu/CA catalyst. Then, this intermediate is oxidized by the generated reactive radical oxygen species $\bullet\text{OH}$ and $\bullet\text{OOH}$ from the activation of H_2O_2 over Cu/CA to give the desired formamide product along with the release of H_2O .

We developed an efficient heterogeneous copper catalyst for the synthesis of formamides *via* the oxidative carbonylation of amines with inexpensive and easily accessible paraformaldehyde as the carbonyl source under base-free conditions. To the best of our knowledge, this is the first active heterogeneous non-noble-metal catalytic system developed without base additives. Our system exhibits a good amine substrate scope and different aromatic and aliphatic amines are well tolerated. In comparison with previous systems, our system shows impressive advantages such as a low reaction temperature (50 °C), green solvent (H_2O), inexpensive and recyclable catalyst (supported Cu catalyst) and a sustainable catalyst support (cellulose-derived biochar support). EPR spin trapping and control experiments reveal that $\bullet\text{OH}$ and $\bullet\text{OOH}$ radicals behave as, respectively, minor and major reactive oxygen species in the

reaction. Our work not only advances the sustainable synthesis of formamides but also demonstrates a new application of biochar derived from biobased feedstock, namely for preparing heterogeneous catalytic materials.

This work is supported by the Strategic Priority Research Program of the Chinese Academy of Sciences (Grant No. XDB1500203), National Natural Sciences Foundation of China (22572202), and Gansu Science and Technology Major Project (24ZD13FA002).

Conflicts of interest

There are no conflicts to declare.

Data availability

The data supporting this article have been included as part of the supplementary information (SI). Supplementary information is available. See DOI: <https://doi.org/10.1039/d5cc06007a>.

Notes and references

- H. Bipp and H. Kieczka, *Ullmann's Encyclopedia of Industrial Chemistry*, 2011.
- Y. Zou, Z. Ma, L. Dong, Y. Yang, P. Wang, S. Sheng, R. Zbořil, R. V. Jagadeesh, Z. Chen, *Coord. Chem. Rev.*, 2025, 541, 216750.
- J. Omprakash Rath and G. Subray Shankarling, *ChemistrySelect*, 2020, 5, 6861.
- S. B. Jagtap and S. B. Tsogoeva, *Chem. Commun.*, 2006, 4747.
- C. J. Gerack and L. McElwee-White, *Molecules*, 2014, 19, 7689.
- D. Jiao, J. An, H. Li, Z. Huang, Y. Wang and F. Wang, *Chin. J. Catal.*, 2023, 53, 161.
- X.-H. Cai, S.-q. Cai and B. Xie, *Curr. Org. Chem.*, 2021, 25, 223.
- J. Muzart, *Molecules*, 2021, 26, 6374.
- Q.-W. Song, R. Ma, P. Liu, K. Zhang and L.-N. He, *Green Chem.*, 2023, 25, 6538.
- G. Sivakumar, R. Kumar, V. Yadav, V. Gupta and E. Balaraman, *ACS Catal.*, 2023, 13, 15013.
- W. Li and X.-F. Wu, *Adv. Synth. Catal.*, 2015, 357, 3393.
- X. Dai, J. Rabeah, H. Yuan, A. Brückner, X. Cui and F. Shi, *ChemSusChem*, 2016, 9, 3133.
- S. Atpadkar and M. S. Gill, *Synthesis*, 2024, 1449–1459.
- X. Dai and J. Rabeah, *ChemCatChem*, 2025, 17, e202500359.
- B. Xu, L. Zhou, R. J. Madix and C. M. Friend, *Angew. Chem., Int. Ed.*, 2010, 49, 394.
- L. Zhou, C. G. Freyschlag, B. Xu, C. M. Friend and R. J. Madix, *Chem. Commun.*, 2010, 46, 704.
- O. Saidi, M. J. Bamford, A. J. Blacker, J. Lynch, S. P. Marsden, P. Plucinski, R. J. Watson and J. M. J. Williams, *Tetrahedron Lett.*, 2010, 51, 5804.
- I. Metaxas, E. Vasilikogiannaki and M. Stratakis, *Nanomaterials*, 2017, 7, 440.
- Z. Ke, Y. Zhang, X. Cui and F. Shi, *Green Chem.*, 2016, 18, 808.
- N. Shah, E. Gravel, D. V. Jawale, E. Doris and I. N. N. Namboothiri, *ChemCatChem*, 2014, 6, 2201.
- G.-L. Li, K. K.-Y. Kung and M.-K. Wong, *Chem. Commun.*, 2012, 48, 4112.
- P. Preedasuriyachai, H. Kitahara, W. Chavasiri and H. Sakurai, *Chem. Lett.*, 2010, 39, 1174.
- M. C. Pichardo, G. Tavakoli, J. E. Armstrong, T. Wilczek, B. E. Thomas and M. H. G. Precht, *ChemSusChem*, 2020, 13, 882.
- L. Wang, Y. Hu, Q. Pu, Y. Yao, H. Zhang, Y. Guo, Y. Li, B. Dai and Z. Ke, *RSC Sustain.*, 2025, 3, 395.
- X.-Y. Liu, M. Huang, H.-L. Ma, Z.-Q. Zhang, J.-M. Gao, Y.-L. Zhu, X.-J. Han and X.-Y. Guo, *Molecules*, 2010, 15, 7188.

- 26 Y. Sohn, D. Pradhan, L. Zhao and K. T. Leung, *Electrochem. Solid-State Lett.*, 2012, **15**, K35.
- 27 H. Qi, S. Mao, J. Rabeah, R. Qu, N. Yang, Z. Chen, F. Bourriquen, J. Yang, J. Li, K. Junge and M. Beller, *Angew. Chem., Int. Ed.*, 2023, **62**, e202311913.
- 28 C. Xie, L. Lin, L. Huang, Z. Wang, Z. Jiang, Z. Zhang and B. Han, *Nat. Commun.*, 2021, **12**, 4823.
- 29 K. Makino, T. Hagiwara and A. Murakami, *Int. J. Radiat. Appl. Instrum., Part C Radiat. Phys. Chem.*, 1991, **37**, 657.